

This article was downloaded by:

On: 22 January 2011

Access details: *Access Details: Free Access*

Publisher *Taylor & Francis*

Informa Ltd Registered in England and Wales Registered Number: 1072954 Registered office: Mortimer House, 37-41 Mortimer Street, London W1T 3JH, UK



The Journal of Adhesion

Publication details, including instructions for authors and subscription information:

<http://www.informaworld.com/smpp/title~content=t713453635>

The Role of Adhesion Promoters on the Molecular and Mesoscopic Structure of the Interphase

M. Grunze^a; A. Schertel^a; R. Uhrig^a; A. Welle^a; Ch. Wöll^a; T. Strunskus^b

^a Universität Heidelberg, Lehrstuhl für Angewandte Physikalische Chemie, Heidelberg, Germany ^b Technische Fakultät der Christian-Albrechts-Univ. zu Kiel, Kiel-Gaarden, Germany

To cite this Article Grunze, M. , Schertel, A. , Uhrig, R. , Welle, A. , Wöll, Ch. and Strunskus, T.(1996) 'The Role of Adhesion Promoters on the Molecular and Mesoscopic Structure of the Interphase', *The Journal of Adhesion*, 58: 1, 43 – 67

To link to this Article: DOI: 10.1080/00218469608014399

URL: <http://dx.doi.org/10.1080/00218469608014399>

PLEASE SCROLL DOWN FOR ARTICLE

Full terms and conditions of use: <http://www.informaworld.com/terms-and-conditions-of-access.pdf>

This article may be used for research, teaching and private study purposes. Any substantial or systematic reproduction, re-distribution, re-selling, loan or sub-licensing, systematic supply or distribution in any form to anyone is expressly forbidden.

The publisher does not give any warranty express or implied or make any representation that the contents will be complete or accurate or up to date. The accuracy of any instructions, formulae and drug doses should be independently verified with primary sources. The publisher shall not be liable for any loss, actions, claims, proceedings, demand or costs or damages whatsoever or howsoever caused arising directly or indirectly in connection with or arising out of the use of this material.

The Role of Adhesion Promoters on the Molecular and Mesoscopic Structure of the Interphase*

M. GRUNZE,** A. SCHERTEL, R. UHRIG, A. WELLE and CH. WÖLL

Universität Heidelberg, Lehrstuhl für Angewandte Physikalische Chemie, INF 253, D-69120 Heidelberg, Germany

T. STRUNSKUS

Technische Fakultät der Christian-Albrechts-Univ. zu Kiel, Kaiserstr. 2, 24143 Kiel-Gaarden, Germany

(Received March 23, 1995; in final form October 6, 1995)

New experimental results are described from Near Edge X-Ray Absorption Fine Structure (NEXAFS) spectroscopy, X-ray photoelectron spectroscopy (XPS) and Atomic Force Microscopy (AFM) on the molecular orientation, chemical composition, and topography of PMDA/ODA Polyimide (PI) deposited by the Langmuir-Blodgett (LB) technique onto Si (100) surfaces covered with a native oxide (SiO_x) and onto SiO_x substrates pre-treated with a variety of alkylsilanes. The alkylsilane monolayers used as adhesion promoters were found to be chemically and structurally stable during temperature treatments used to imidize the polymer precursor films. On both the oxidized silicon surface and on the silane-treated surfaces, we find a thickness-dependent, preferential orientation of the pyromellitimide unit in PI, but randomly-oriented oxydianiline fragments. We can not identify any specific chemical bonds between the polymer and the aminosilane film or, in the case of the untreated surface, the SiO_x substrate. However, a quantitative analysis of the NEXAFS data reveals a pronounced deficit in oxydianiline in the monolayer (ML) films, which decreases with film thickness, and a higher degree of imidization on the 3-aminopropyltrimethoxysilane (APS) surface indicating that imide linkages are formed between the polymer and the aminosilane. The AFM images show a heterogeneous surface topography with nucleation of PI polycondensates on both the SiO_x and aminosilane-treated surfaces. On the aminosilane surface additional nuclei are detected, believed to be polycondensates of aminosilane formed during imidization of the PI precursor. Nucleation of aminosilane polycondensates is not observed in the absence of polyamic acid. As suggested by a comparison of Lateral Force Microscopy (LFM) and Atomic Force Microscopy measurements, these aminosilane nuclei are covered by PI with increasing film thickness and, hence, provide mechanical connections between the polymer and substrate on a mesoscopic scale. Delamination experiments of 2 μm thick PI films spun onto ω -amino and methyl terminated alkylsilanes indicate that bond fracture always occurs in the aminosilane/PI and alkylsilane/PI and interphase. We conclude that the adhesion promotion effect of LB-deposited polyimide films by aminosilanes can be explained by chemical stabilization of the interface against decomposition and mechanical interlinking surface via polycondensates of aminosilane on a mesoscopic length scale. Our study is not conclusive as to whether covalent bonding of the polymer to the substrate via the silane is important for macroscopic adhesion.

KEY WORDS: Adhesion promoters; AFM; aminosilanes; interphase; NEXAFS; polyimide; silanes; XPS

* One of a Collection of papers honoring Jacques Schultz, the recipient in February 1995 of *The Adhesion Society Award for Excellence in Adhesion Science, Sponsored by 3 M.*

** Corresponding author.

Table of Acronyms and Abbreviations

AFM	Atomic force microscopy
AHTMS	17-Aminohexadecyl-trimethoxy-silane
APE	3-Aminopropyl-triethoxysilane
APS	3-Aminopropyl-trimethoxysilane
LB	Langmuir Blodgett
LFM	Lateral force microscopy
ML	Monolayer
NEXAFS	Near edge X-ray absorption fine structure spectroscopy
ODA	4,4'-Oxydianiline
OTMS	Octadecyltrimethoxysilane
OTS	n-octadecyltrichlorosilane
PI	Polyimide
PMDA	Pyromellitic dianhydride
PTS	n-propyl-trimethoxysilane
XPS	X-ray photoelectron spectroscopy

1. INTRODUCTION

A recent article by Brochard-Wyart *et al.*¹ discusses the important factors for adhesion promotion between a flat solid and a rubber by (chemically identical) connector molecules. The importance of interdigitation on a molecular length scale of the connector molecules grafted onto the surface and the rubber is pointed out, as well as the increase in adhesion energy gained by chemical bonds between the substrate and the rubber via the connector molecules. Best adhesion is achieved when both criteria are met, interdigitation and chemical bonding.

There is, however, a wide class of glassy or partly-crystalline polymers where these concepts are not directly adaptable. The polymer or the polymer precursor itself can have a high chemical reactivity towards the substrate, leading to polymer fragmentation and corrosion of the substrate and formation of a structurally and chemically ill-defined "weak boundary layer" which is detrimental to adhesion. A frequent observation in delaminated bonds between PI (the model system studied here) and an inorganic substrate is that cohesive failure occurred in the *interphase* between the bulk of the two materials. For example, Oh *et al.*² studied the peel strengths of PIs on SiO₂, Al₂O₃ and MgO and related these measurements to XPS and SEM results on the delaminated surfaces. In all cases, a cohesive failure in the "weak boundary layer" located about 2 nm from the inorganic substrate into the PI film was observed. We suggested³ that PI decomposition at the interface and the substrate-induced orientation of the polymer chains in the interphase, relative to their bulk orientation, will lead to a region of reduced density and hence cohesive strength.

To eliminate strong chemical reactions between the polymer and the inorganic surface, the substrate can be chemically passivated (which in turn also reduces chemical bonding at the interface) or a suitable spacer molecule, which itself is not degraded by a reactive substrate, can be applied to the substrate. Typical spacer molecules for PI, and

a wide class of technically important polymers, are derivatized short alkylsilanes $R(CH_2)_nSi(OCH_3)_3$ ($n < 4$), which bond to the substrate via their trimethoxy or triethoxy head group, and presumably to the polymer via their chemically reactive tail groups (R). For example, for thick polymerized APS films it has been shown that interdiffusion of a polymer with the silane leads to improved adhesion⁴. Oh *et al.*⁵ reported an improvement in "adhesion" strength when APE was applied to the silicon wafer prior to spin coating of the PI precursor. The locus of failure in delamination experiments was still found to be in the PI, although the peel strength was increased by a factor of 1.5–2.0, depending on total film thickness. The same increase in peel strength was also found by Greenblatt *et al.*⁶ for APE and N,N-dimethyl-3-aminopropyltriethoxysilane. They noted that the adhesion promotion effect of the latter is obscure, since the molecule is not expected to react with the polymer. Interestingly, for N-methyl-3-aminopropyltriethoxysilane, which also reacts with polyamic acid, the increase in peel strength was smaller than for the two other compounds. No adhesion promotion was observed in this study for the methyl terminated n-butyl-trimethoxysilane. The difference between APE and N-methyl-3-aminopropyltriethoxysilane was interpreted to be a result of stable imide formation between polymer and silane for the amine compound, and thermally unstable diamide formation or steric hindrance for imide formation for the N-methyl compound, respectively (compare Figs. 1 and 4 in Ref. 6.) Buchwalter⁴ suggested, in her comprehensive review on adhesion of PI to metals and ceramics, that with the adhesion promoter the interfacial region within the PI is less oriented and more entangled than the same system without the adhesion promoter, resulting in a mechanically stronger interface. As we will show in this work, the first suggestion is not supported by our model studies, whereas the notion of increased entanglement, although not on a molecular but rather mesoscopic scale, is consistent with our AFM and LFM results.

The best-defined method available to study the orientation of the polymer molecule as a function of distance from a solid interface is by preparing films of defined thickness in a layer-by-layer fashion using the Langmuir Blodgett technique^{7,8,9}. Our previous Near Edge X-ray Absorption Fine Structure (NEXAFS) measurements on PI films deposited by the LB technique onto etched silicon, gold and silver revealed that the orientation in the interphase depends on the chemical bond between the substrate and the polymer, *i.e.* the nature and reactivity of the substrate surface³. A high degree of orientation in the polymer layers was observed on gold and silver surfaces. In our previously reported XPS results⁸ we concluded that electrostatic interactions between PI and gold, and formation of mono- or bidentate type bonds on the silver substrate, facilitate bonding. On all substrates, an orientation close to the bulk of PI is found for a 5-layer deposit, *i.e.* at a distance of ~ 3 nm away from the surface.

In contrast to the high degree of order on gold and silver surfaces, the interfacial reaction on etched Si (100) effectively inhibits cycloimidization in the first layer and causes a deviation from stoichiometric PI exceeding a thickness of 3 MLs, leading to a strong disturbance of the layered structure³. These structural results on Si (100) correlate to preliminary delamination experiments on the LB-deposited PI films on Si (100)⁹ which show delamination in the interphase between substrate and polymer.

In this paper, we amplify the hypothesis that the structural properties of the "interphase" between polymer and inorganic substrate play an important (if not

decisive) role for the stability of the adhesive bond. We describe new experiments on the temperature-dependent behavior of aminosilane films used as adhesion promoters, and the chemical composition of PI films on silicon surfaces covered with a thin oxide layer or treated with an aminosilane. For the first time, we correlate information on the molecular chemistry and structure with topographic images on a mesoscopic scale, and suggest that both length scales could be important for macroscopic adhesion strength in our model system. The results obtained in our studies do not disprove previous models for the role of aminosilane adhesion promoters, but should stimulate further detailed work on these technologically relevant systems. The experiments described here are complemented by delamination experiments of PI films prepared by spin coating onto silane-pretreated silicon surfaces.

2. EXPERIMENTAL

All substrates were cut from Si (100) wafers. Prior to film preparation the substrates were cleaned by a wet chemical treatment in a freshly-prepared hot acid mixture (Piranha solution, H_2SO_4 (conc.) : H_2O_2 (30%) = 3 : 1) for one hour followed by an extensive rinse with ultra clean water (Millipore) and drying in nitrogen. Exposure to the ambient led to formation of a native oxide layer. ML silane film preparation was performed by immersing the Si-substrates in a solution of 1 mmol/l APS (ABCR Company) in ethanol for about 24 h or in a solution of 1 mmol/l OTS (Merck), or 1 mmol/l PTS in bicyclohexyl (Fluka). To remove excess silane aggregates resulting from polymerization in solution, the samples were rinsed with Millipore water and stirred in a chloroform bath for several minutes. They were then wiped with a soft 100% cotton cloth, which had been dipped in chloroform, and blown dry with nitrogen.

Our procedures for the deposition and imidization of the octadecylammonium salt of polyamic acid by the LB technique are described elsewhere^{3,7,8}. For each substrate surface (native oxide on Si or aminopropylsilane treated SiO_x), three different types of samples consisting of 1, 3 and 5 MLs of the PI precursor, polyamic acid, were prepared.

Delamination experiments with spun-on films were carried out with wafers coated with APS, OTS and PTS^{1,2}. These silane layers were prepared identically to those used in the NEXAFS, XPS, and AFM experiments. They were characterized extensively in our laboratory¹⁰⁻¹². Note that, contrary to the industrial application process, only ML silane films were used for the investigation of the PI interphase structure and chemistry.

For the NEXAFS experiments the polyamic acid films were stored in a sealed container in air before being analyzed at the synchrotron radiation facility BESSY in Berlin. After introduction into the multi-technique UHV analysis chamber by help of an air-lock and a transfer system, the films were investigated by NEXAFS (see below) and with XPS. Imidization was carried out subsequently in vacuum by a temperature treatment consisting of heating to 523 K for 30 min or 573 K for 40 min.

In a NEXAFS experiment, the excitation of electrons into unoccupied molecular orbitals via dipole transition from core levels is probed¹⁴. The variation of the NEXAFS spectra for different orientations of the polarization vector of the incident radiation is used to determine the *average* orientation of a particular functional group in the polymer molecule. For a transition from a core level X (X = C1s, N1s, O1s) into a

molecular orbital, Φ_v , the transition probability, I_v , is given by:

$$I_v(\Theta) = 1/3 |T_{X,\Phi_v}|^2 \times (1 + 1/2(3\cos^2\Theta - 1) \times (3\cos^2\tau - 1)), \quad (1)$$

where Θ is the angle of incidence of the X-ray photons and τ the tilt-angle of the transition dipole moment, T_{X,Φ_v} , with respect to the surface normal¹⁴. A random azimuthal orientation of the molecules is assumed. Note that, according to Eq. (1) for a tilt angle of $\tau = 54.7^\circ$ of the molecular transition dipole moment, no angular variation is expected even for a well-ordered overlayer, as for a random molecular orientation. Also, for an angle of incidence of $\Theta = 54.7^\circ$ ("magic angle") all molecular tilt-angles will give the same excitation probability. For Eq. (1) a degree of polarization in the plane of the synchrotron of 100% is assumed and corrections are needed for smaller degrees of polarization¹⁴, which also slightly modify the two angles discussed above. In our data analysis the measured degree of polarization of 85% was used.

The BESSY experiments were carried out with a resolution of better than 0.8 eV at the C1s-edge. The angle of incidence of the X-ray photons was varied from 90° (E-vector in the surface plane-normal incidence) to 20° (E-vector parallel to the surface normal-grazing incidence) in steps of 10° . The samples were aligned using the bright zero-order (specular) diffraction beam of the monochromator. The diameter of the synchrotron beam spot on the sample is approximately 1.5 mm. At grazing incidence, however, the spot is substantially elongated (approx. 4.5 mm at 20°). Calibration of the energy scale was performed by recording the Au 4d and Cu 2p absorption edges in the first and second order. All spectra were taken in the partial yield mode using a retarding voltage of -150 V at the detector. The NEXAFS spectra were normalized to the incident photon flux by dividing the raw data by the monochromator transmission function, which had been determined for freshly-sputtered, clean gold and silver surfaces. The acquisition time of each spectrum was 5 min. The base pressure in the main chamber was always better than 2×10^{-7} Pa. All spectra were taken at room temperature.

The thermal stability of the silane films was investigated in a modified Leybold-Heraeus LHS-11 system. The examination of the delaminated surfaces of PI spin-coated onto silane-treated wafers was carried out with the VG ESCASCOPE photoelectron microscope in the small spot mode with a field of view of $50 \mu\text{m}$.

AFM measurements were performed with a Park Scientific Autoprobe CP System with a $5 \mu\text{m}$ scanner and an LFM (Lateral Force Microscopy) head using Ultralevers. The scan rate was 2 Hz in the constant force mode with a force of 44.8 nN. Topographic scans with forces as low as 4.5 nN showed no difference. Images displayed below are not filtered or manipulated in any way. The samples studied by AFM are those analyzed before with NEXAFS and XPS; between the experiments, they were stored in cleaned plastic containers.

3. RESULTS

3.1 Structure and Thermal Stability of Aminosilane Films

A comparison of the growth kinetics, lateral order and of the orientation of aminosilane the molecules in self-assembled MLs shows that, contrary to methyl-terminated

alkylsilanes¹⁰⁻¹², the amino-terminated silane films have a high degree of disorder. The XPS signal of a high binding energy shoulder at $E_B = 402.5$ eV is assigned to protonated nitrogen of the amino groups¹⁰ interacting via acid-base interactions with the substrate hydroxyl groups and/or intra- and intermolecular acid-base interactions in the aminosilane layer. The high degree of disorder is also evident from contact angle, NEXAFS, and ellipsometric measurements^{10,12}.

Important for the interpretation of the results obtained for the LB films deposited onto silane MLs is their stability during the heat treatment applied to imidize the film. In Figure 1 the integrated intensities of the C 1s, O 1s and N 1s emission corrected for photoionization cross section and analyzer transmission are displayed for APS and OTS films as a function of annealing temperature in vacuum. Up to 550 K there is no evidence for fragmentation or desorption in the C 1s, O 1s or Si 2p spectra of APS; the small decrease in C 1s intensity and increase in Si 2p and O 1s intensity by approx. 20% in the OTS data results from the desorption of (presumably) excess material not removed in the wiping and rinsing process^{10,12}. The average film thickness for APS calculated from the attenuation of the Si 2p signal is about 0.4 nm, which is considerably less than expected from a geometrical model of an ordered APS layer (0.85 nm). For OTS, the difference in the geometrical model is within the noise of the data, *i.e.* 2.7 nm at 300 K. If we calculate the thickness of the APS layer by ratioing the C 1s signal of APS to the C 1s signal of OTS, an average thickness of the APS film of 1.05 nm would be obtained. This difference in estimated thickness of the APS layer can be explained by the disorder in the films, since the attenuation of the Si 2p substrate signal by the film is

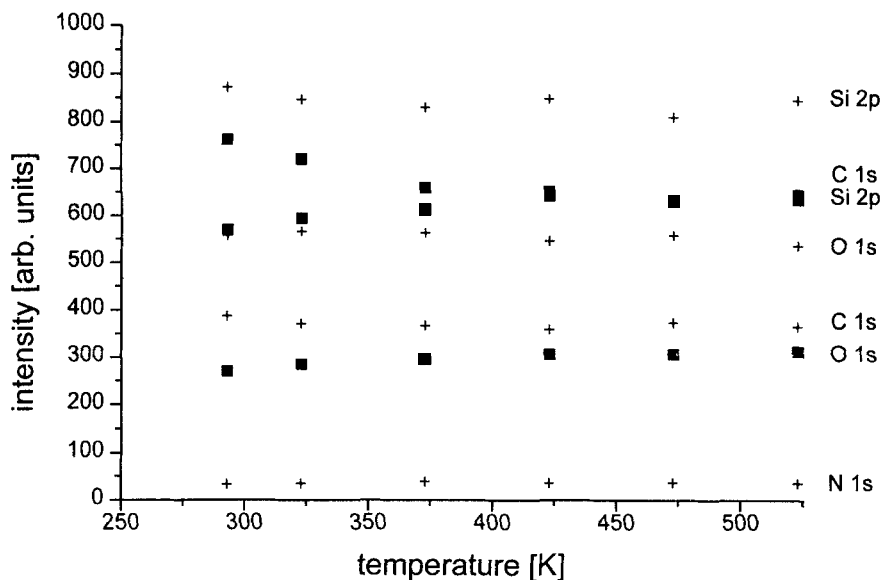


FIGURE 1 Integrated C 1s, Si 2p XPS spectra for octadecyltrichlorosilane (OTS) (squares) and 3-aminopropyltrimethoxysilane (APS) (crosses) after annealing at the indicated temperatures in ultra-high vacuum. For APS the integrated N 1s intensity is also displayed.

obscured by the silane groups of APS not bonded to the SiO_x surface. Hence, taking the intensity of the OTS carbon signal and the OTS film thickness as a reference for the APS C 1s signal, a reasonable value for the ML film is obtained.

Furthermore, the stoichiometry for the APS layers deviates considerably from the expected value even directly after film deposition. The concentration of the amino groups is only about one third of the signal expected for stoichiometric APS. In previous work, we noted the strong X-ray sensitivity of APS films in XPS measurements, but can exclude such an effect in the present data. Approximately the same amino-nitrogen deficit was found on all APS samples studied in our laboratory (about 20 different samples).

A surprising but important effect for adhesion promotion by aminosilanes is observed in the XPS data in Figure 2 recorded after annealing the APS layers at 523 K. The spectrum recorded at 291 K exhibits the typical high binding energy shoulder for protonated nitrogen at $E_B = 402.5$ eV. However, heating the film in vacuum to 523 K, the imidization temperature of polyamic acid, leads to the irreversible decrease of the high binding energy shoulder indicating the conversion of protonated to free amino

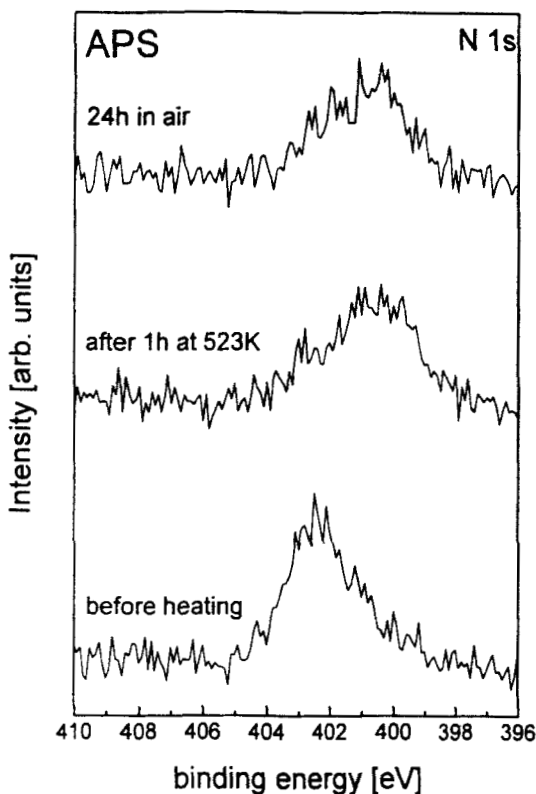


FIGURE 2 N 1s data of (a) a 3-aminopropyltrimethoxysilane (APS) ML film after deposition; (b) after annealing in ultra high vacuum for 1 h to 523 K, (c) after exposure of the annealed film to air at 291 K for 24 h.

groups in the film. Hence, at temperatures where the octadecylammonium salt in the polyamic acid layers decomposes and imidization is initiated⁷, more free amino functionalities are available for bond formation between the silane “connector” molecules and the polymer. Figure 2c shows that the annealed films are reasonably stable during storage in the ambient for 24 h. Whether or not heating in vacuum improves the molecular order in these films has not been studied yet.

We note that this behavior is different from the observations that we reported previously on multilayer films, in which heating in air caused dewetting of the silane and formation of large polycondensates on the surface¹¹. These previous measurements were done on films, which were adsorbed from ethanol solution, rinsed with ethanol, and not wiped with a cotton cloth as in the present data. In the ML films used in this study, we could not find evidence for dewetting in AFM measurements after heating in vacuum.

3.2 Structural Studies of Langmuir-Blodgett Deposited PI Films

In Figure 3, we compare the N 1s (see Fig. 3(a)) and C 1s (see Fig. 3(b)) NEXAFS data for LB-deposited PI films on SiO_x and APS treated silicon surfaces with those previously obtained on clean hydrophobic silicon surfaces³. The assignment of the various C 1s and N 1s edge excitations in the spectra in Figure 3 is given in Ref. 3. As discussed in detail before, the latter show a high distortion and fragmentation over at least three MLs⁵. During imidization, fragmentation occurs in the interphase leading to a degraded polymer layer. This was first concluded from XPS studies⁷, and later by the NEXAFS experiments reproduced in Figure 3³. The NEXAFS C 1s and N 1s spectra for the 1 LB-layer film on Si (100) are not representative for PI and exhibit a different angular behavior than expected for intact PI. In contrast to the films on Au³, Ag³, and the SiO_x and APS-treated substrates shown here, the C 1s spectra on clean Si (100) show a stronger absorption at normal than at grazing incidence, *e.g.* the average molecular orientation of the phenyl rings in the polymer fragments is steeper than the “magic angle” of 54.7°. From the N 1s data, an average tilt angle of the pyromellitimide unit of *ca.* 60° with respect to the substrate plane is obtained³. We concluded³ that the interfacial reaction inhibits cycloimidization in the first layer and causes fragmentation of the polymer. The deviation in the C 1s-edge data from stoichiometric PI is also observed for the 3 and 5 LB-layer films on Si (100); the intensity ratio of the two N 1s - π^* resonances at 401.8 and 404.3 eV, however, are consistent with the presence of imide nitrogen. The C 1s and N 1s data can be explained by fragmentation and partial desorption of the oxydianiline part of the polymer with the pyromellitimide fragment remaining attached to the surface layer.

The NEXAFS data for PI on SiO_x and the APS-treated surface are distinctly different from those on the clean Si (100) surface. The N 1s ML spectra resemble closely the spectra for intact PI (compare the 5 ML data) and have an angular dependence consistent with a preferential orientation of the pyromellitimide unit of 34° (SiO_x) and 38° (APS) relative to the surface normal, respectively. Note, however, that the total absorption intensity on the APS-treated surfaces at photon energies greater than the absorption edge (405.8 eV) is larger than on the SiO_x surface because of the presence of APS. Aminosilane N 1s NEXAFS spectra themselves show no angular dependence due

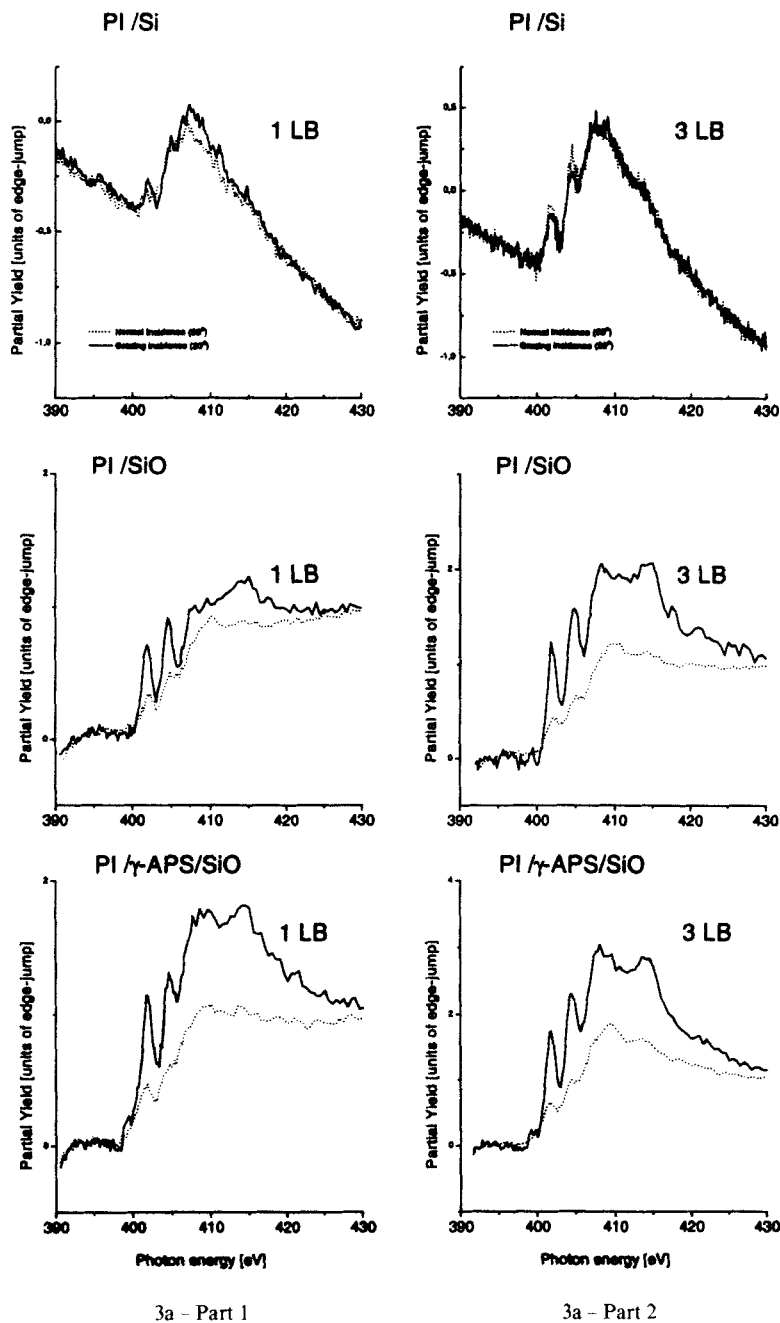


FIGURE 3 (a) N 1s NEXAFS data and (b) C 1s NEXAFS data for the 1, 3 and 5 ML LB-deposited PI films on an etched Si surface, a Si surface covered with a native oxide (SiO₂) and a (SiO₂) surface covered with a ML film of 3-aminopropyltrimethoxysilane (APS). Dashed line: Normal incidence (90°). Solid line: Grazing incidence (20°). See text for discussion.

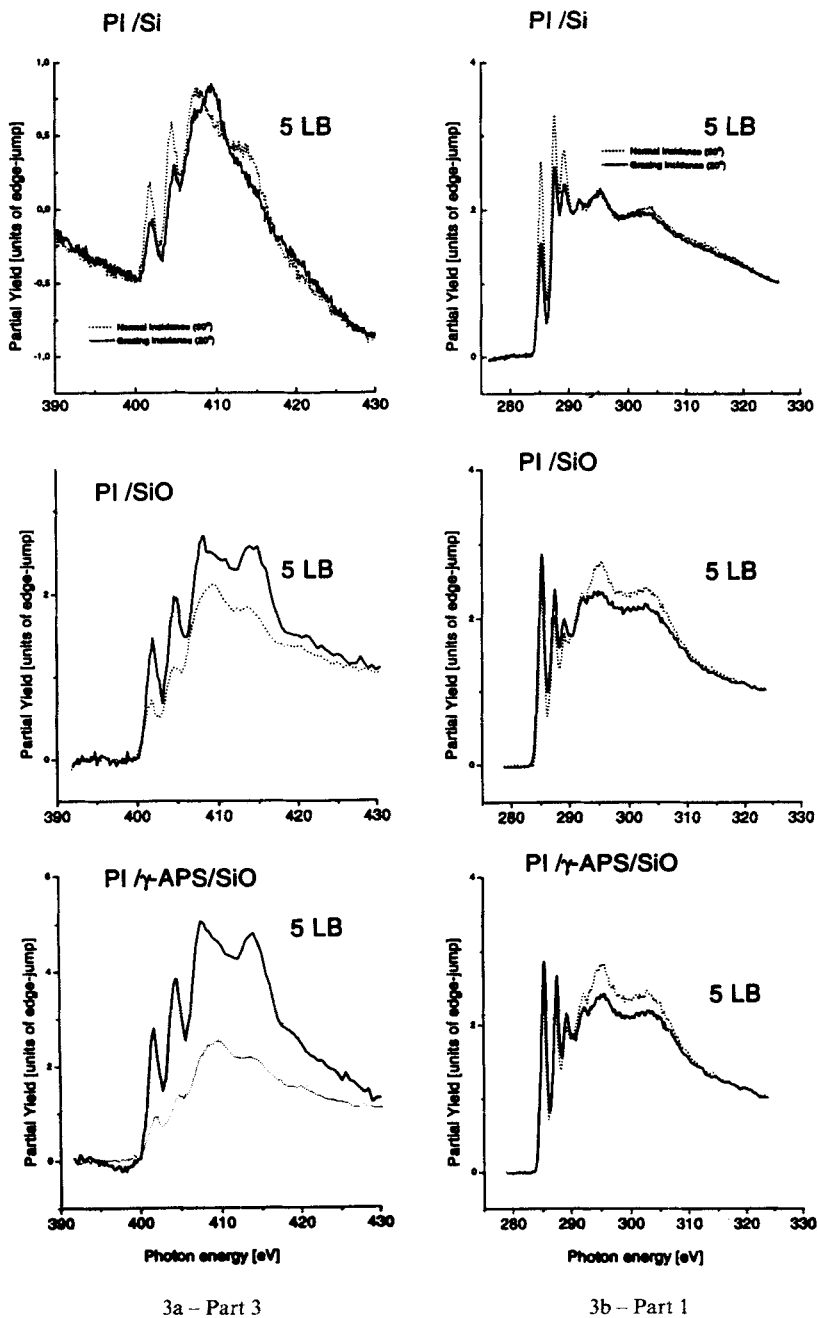
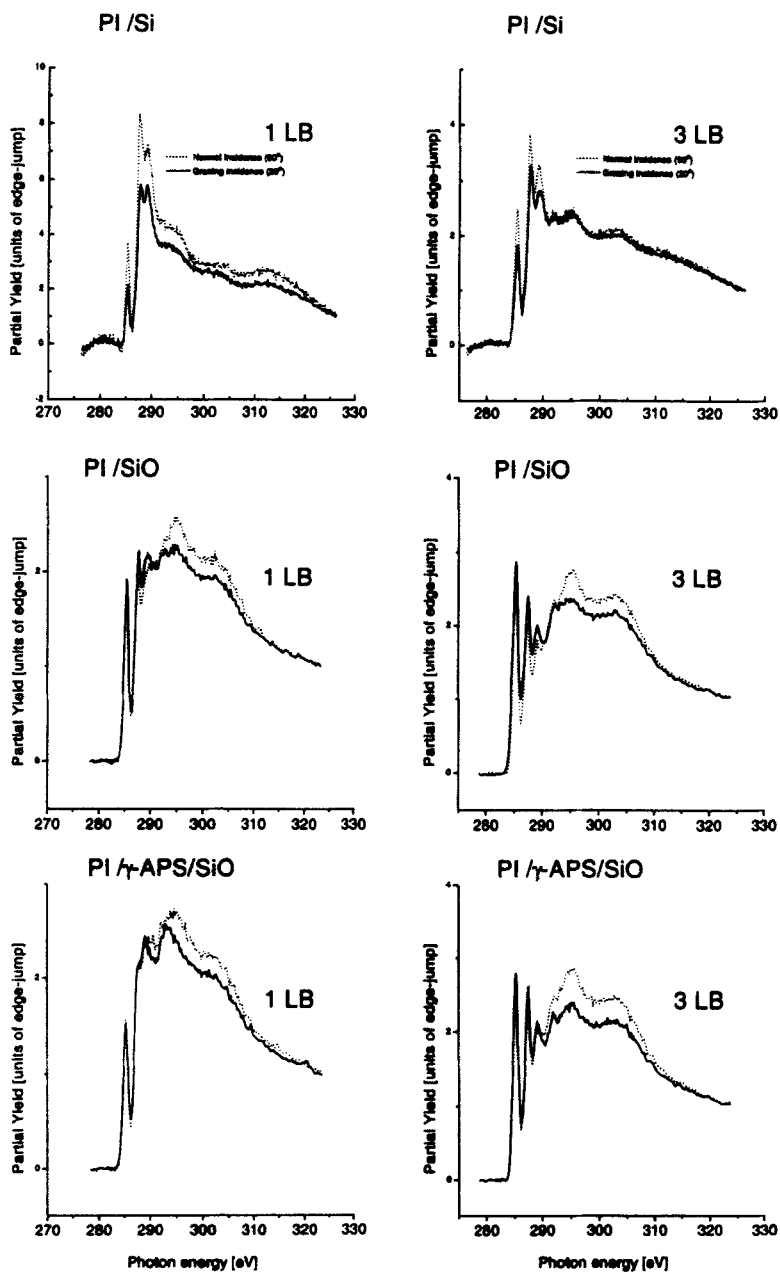


FIGURE 3 (Continued)



3b - Part 2

3b - Part 3

FIGURE 3 (Continued)

to their disorder¹⁰. The comparison between the data on the bare and APS-treated substrate demonstrate that the spectra are dominated by the PI deposit. On both surfaces, no evidence for a interfacial reaction preventing imidization of the pyromellitimide unit can be detected.

With increasing film thickness the N 1s data on the two surfaces more closely resemble each other since the signal from the silane layer is progressively more attenuated. The angular behavior remains pronounced; the calculated values for the tilt angles are listed in Table I. On both surfaces the tilt angle increases slightly with increasing film thickness and the data become similar to those of thick PI films³.

The situation with the C 1s spectra is different: First, the angular behavior for the two substrates and the three film thicknesses is much smaller than for the N 1s data. The dominant feature at 285.2 eV is mainly due to a C 1s- π^* (phenyl) transition in the oxydianiline part, and the transition at 287.4 eV is dominated by the C 1s- π^* (CO) transition in the pyromellitimide part of the polymer. The angular behavior of the 285.4 eV transition indicates a steeper tilt angle relative to the surface plane (closer to 54.7°) of the oxydianiline moiety than for the pyromellitimide unit of the polymer (see Table I). Secondly, the 1-LB data for the two substrates exhibit a loss of the C 1s- π^* (phenyl) ODA transition when compared with the data for the 3 and 5 LB-layer films, revealing a loss of ODA. The C 1s spectra of the 3 and 5 layer films appear representative of intact and stoichiometric PI, when the attenuated additional intensity of the underlying silane film in the APS data is taken into account.

In Figure 4a, we have plotted the C 1s- π^* (phenyl) ODA and 401.8 eV N 1s- π^* (CO) absorption intensities *normalized to the absorption edge height* (an absolute measure for all carbon and nitrogen atoms on the surface) for the MLs and for the 3 and 5 LB-layer films. The normalized C 1s 285.2 eV resonance intensity is a measure for the amount of ODA groups relative to the total carbon concentration, and the N 1s 401.8 eV resonance is a relative measure for the amount of imide nitrogen. Unfortunately, the N 1s edge of the 1 and 3 LB-layer PI on APS cannot be taken as a direct measure of imide nitrogen, since the underlying APS also has a absorption band in the same energy range. At the C 1s edge, the first absorption resonance of APS is well separated at 288 eV, and does not interfere with the 285.2 eV ODA resonance.

TABLE I

Average tilt angle between the surface normal and the normal of the plane of the phenyl rings of the pyromellitimide and between the surface normal and the mean plane of the phenyl rings of the oxydianiline system. (0° corresponds to rings lying flat on the surface).

	pyromellitimide unit (N 1s edge)	oxydianiline unit (C 1s edge)
1 LB Si	34°	55°
3 LB Si	35°	52°
5 LB Si	42°	54°
1 LB APS/Si	38°	56°
3 LB APS/Si	35°	52°
5 LB APS/Si	40°	53°

Errors: $\pm 3^\circ$ absolute

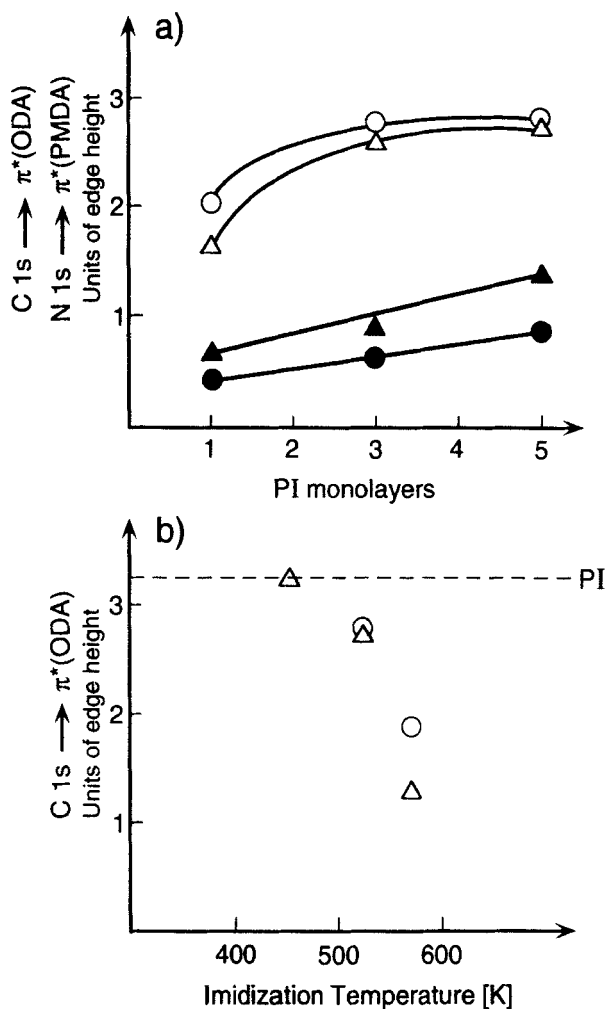


FIGURE 4 (a) Normalized C 1s $-\pi^*(\text{ODA})$, (\bullet , \blacktriangle) and N 1s $-\pi^*(\text{PMDA})$, (\circ , \triangle) NEXAFS data on the SiO_x (\bullet , \circ); and APS (\blacktriangle , \triangle) surface (see text) as a function of film thickness after annealing to 523 K for 30 min. (b) C 1s $-\pi^*(\text{ODA})$ normalized intensities for the 5 ML films on SiO_x (\circ) and APS surfaces (\triangle) as a function of imidization temperature (see text for discussion).

In the MLs we find less ODA than in the 3 and 5 LB-layer films, indicating on both the SiO_x and APS surface a loss of oxydianiline fragments during imidization. The N 1s and C 1s background intensity from the APS layer is successively more attenuated with increasing PI thickness, such that the C 1s absorption intensity for the 5 ML film is dominated by PI and is (within the noise level) identical for the two surfaces. From the N 1s absorption spectra, it follows that the majority of the pyromellitimide units on both surfaces are imidized. Figure 4a shows that the imide concentration relative to total nitrogen increases with film thickness. If we accept that the C 1s and N 1s signals in the 5 LB-layer films on both surfaces are predominantly from PI (see the LFM results

below), the data in Figure 5 reveal that the concentration of pyromellitimide units is higher on the APS surface than on the SiO_x surface. Note however, that both the C 1s and N 1s absorption intensities in Figure 4 do not scale with the number of deposited layers, *i.e.*, PI is lost in the imidization process.

Another important result follows from the plot of the C 1s- π^* (phenyl) ODA intensities for the 5 ML films as a function of imidization temperature in Figure 4b. The data were obtained on different films on the APS-treated and untreated Si (100) native oxide surfaces. With increasing imidization temperature on both surfaces, the C 1s- π^* (phenyl) ODA intensities normalized to the absorption edge are reduced below the value measured for stoichiometric PI. Loss of the polymer is presumably by fragmentation and desorption into the vacuum. Note that at 573 K the relative loss of ODA appears larger on the aminosilane than on the SiO_x surface. This can be explained by

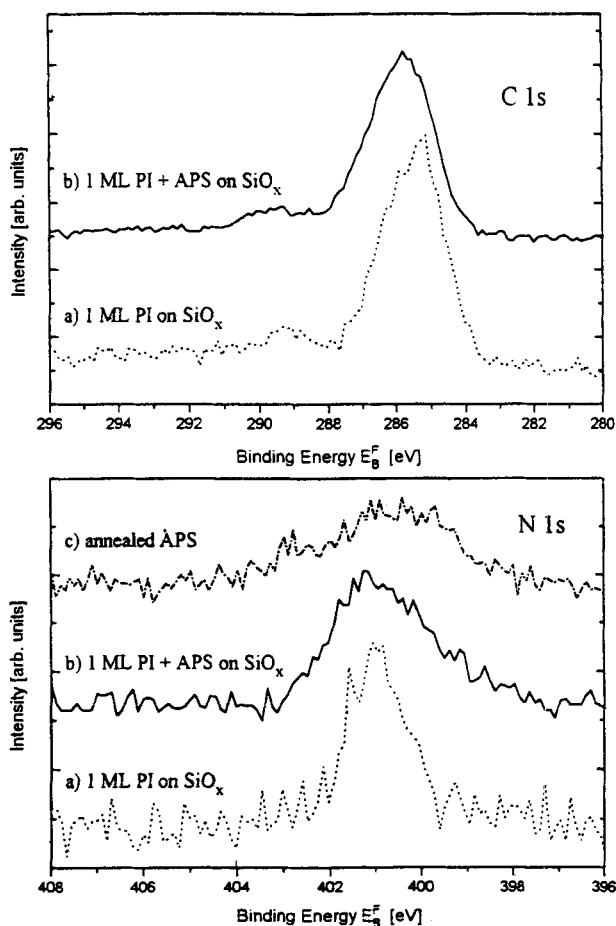


FIGURE 5 C 1s and N 1s XPS data for a 1 ML film, (a) on the SiO_x surface and (b) on the SiO_x surface covered with a ML film of 3-aminopropyltrimethoxysilane (APS). The N 1s spectrum, (c), displays the data of an annealed 3-aminopropyltrimethoxysilane (APS) ML film.

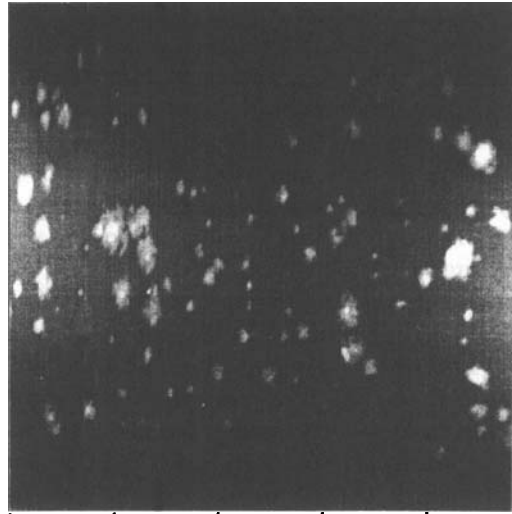
the increase of the C 1s edge on the APS surface due to the increase in signal from the underlying aminosilane film with decreasing film thickness.

The nitrogen edge data are identical for the SiO_x and APS surfaces, considering the signal from the underlying APS layer, and hence not conclusive with respect to chemical bond formation with the substrate. Unfortunately, the XPS data are also inconclusive with respect to chemical bonding to the APS layer. Figure 5 displays the XPS data for the ML PI layer on SiO_x and APS. The spectra for 3 and 5 layers are not reproduced, since they are consistent with PI and resemble very closely those reported by us before for 3 and 5 LB-layers of PI on polycrystalline gold and silver surfaces. The C 1s data in the ML spectra clearly show a carbonyl emission intensity that is too weak for stoichiometric PI. A quantitative evaluation, however, is not appropriate, since also on a gold surface, where bonding is purely by dispersive forces, a deviation from the expected band shape of PI is observed due to final state screening of the polymer core holes by the metal electrons⁸. Part of the deviation from a PI spectrum can also be due to residual carbon from the octadecylamine molecules used in the LB deposition process^{7,8}. The C 1s data for the SiO_x and APS surface are the same, except for a slight C 1s binding energy shift in the PI/APS layer caused by the underlying aminosilane film (this shift is not detectable anymore in the 3 ML spectrum).

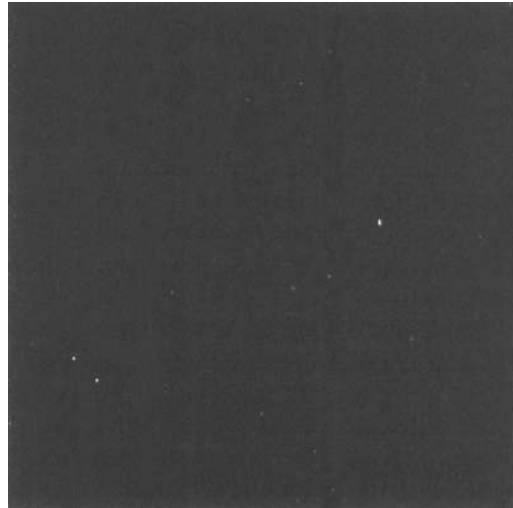
The N 1s XP data of PI on SiO_x show the expected sharp emission for imide nitrogen, which is consistent with imidization of most of the pyromellitimide units. On the APS surface a broader band extending to lower and higher binding energies is measured. In addition to the N 1s spectra for the two PI surfaces, we included the data for an aminosilane film heated in vacuum to 523 K. Within the noise in the data, the PI/APS N 1s spectrum is a combination of the N 1s imide spectrum on SiO_x and the N 1s spectrum of a heated aminosilane film. Hence, neither the NEXAFS nor XPS data show any significant difference between the MLs of PI on SiO_x and APS which could be used to speculate on the nature of bonding between the polymer and the substrate.

The topographic and lateral force images of the 1, 3 and 5 LB-layers on SiO_x and the APS surface are displayed in Figure 6a and 6b, respectively. They clearly show that the PI films annealed at 523 K in vacuum are not homogeneous. The brighter islands have a height of 2.5–4.5 nm on both surfaces, and are believed to consist of PI that forms multilayer islands or coagulates during the imidization process. The surface area covered by these islands increases with the number of deposited polyamic acid layers. The fractional volume, measured from their height and size, scales with 1:2.8:3.2 and 1:2.2:3.2 for the 1,3 and 5 LB-layers on the APS and SiO_x surfaces, respectively. The deviation from the expected ratio of 1:3:5 is consistent with the thickness dependence of the NEXAFS data since the latter technique only probes the topmost polymer layers and does not integrate over the height of the polymer islands.

On the APS surface, additional smaller (max. width 120 nm) and higher (6–9 nm) protrusions are observed; their relative density in the topographic images decreases with PI film thickness. Whereas the islands associated with PI are not, or only weakly, apparent in the lateral force images, the smaller and higher protrusions are detected by their lower friction coefficient as compared with the substrate and PI islands. However, the lateral force contrast is reduced in the 3 ML images, and not observed anymore in the 5 ML films on the APS surface. This also is true for the protrusions on the (dark) substrate surface, suggesting that both substrate surface and the protrusions are

(a) 1 ML PI on SiO_x 

0 1 2 3 4 μm
TOPO image



0 1 2 3 4 μm
LFM image

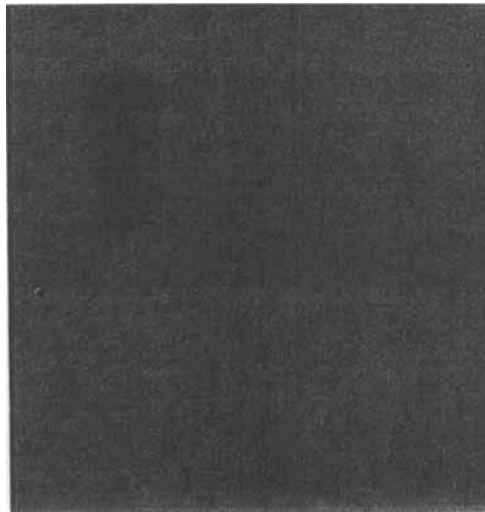
6a - Part 1

FIGURE 6 AFM topographic and lateral force images for the 1, 3 and 5 ML Langmuir Blodgett deposited PI films (a) on the SiO_x surface and (b) on the SiO_x surface covered with a ML film of 3-aminopropyltrimethoxysilane (APS). Grayscale of TOPO images corresponding to 10 nm. See text for discussion.

(a) 3 ML PI on SiO_x



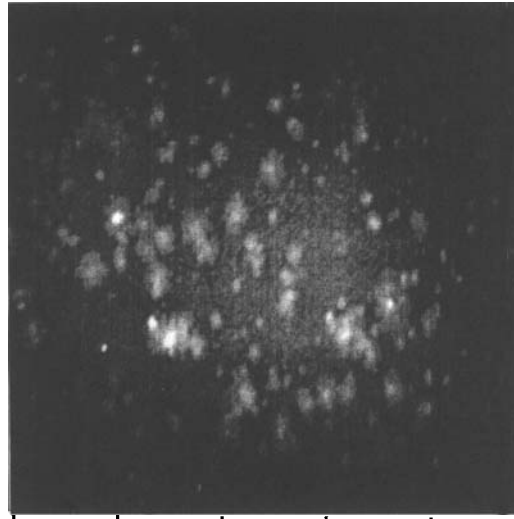
0 1 2 3 4μm
TOPO image



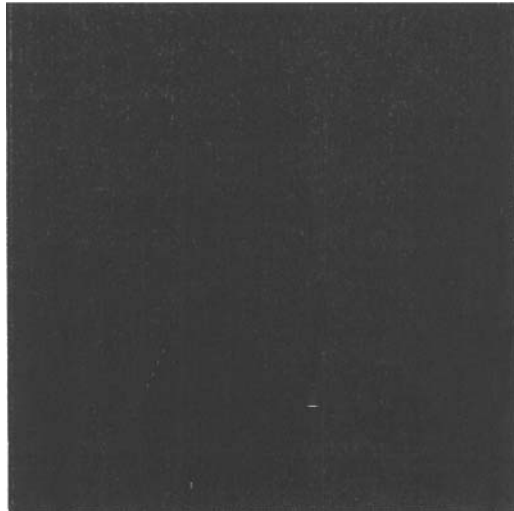
0 1 2 3 4μm
LFM image

6a - Part 2

FIGURE 6 (Continued)

(a) 5 ML PI on SiO_x

0 1 2 3 4 μm
TOPO image

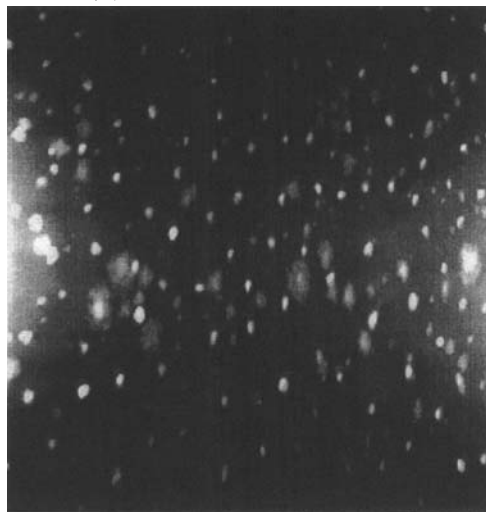


0 1 2 3 4 μm
LFM image

6a - Part 3

FIGURE 6 (Continued)

(b) 1 ML PI, APS, SiO_x



0 1 2 3 4μm
TOPO image

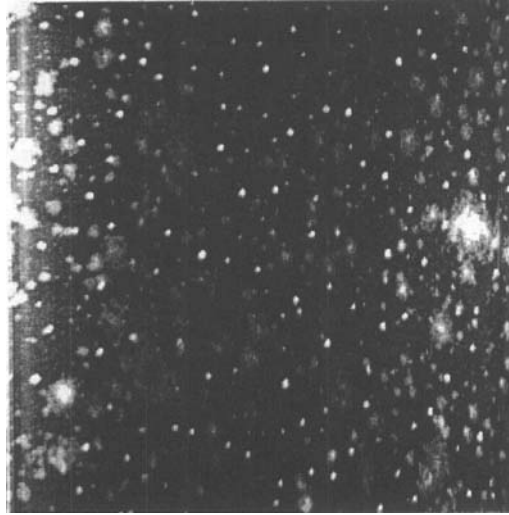


0 1 2 3 4μm
LFM image

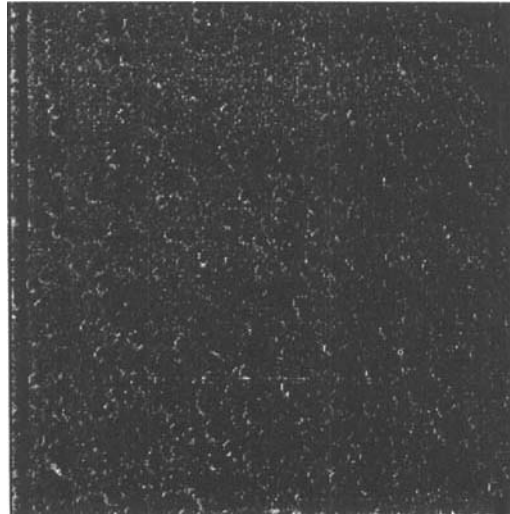
6b - Part 1

FIGURE 6 (Continued)

(b) 3 ML PI, APS, SiO_x



0 1 2 3 4 μm
TOPO image

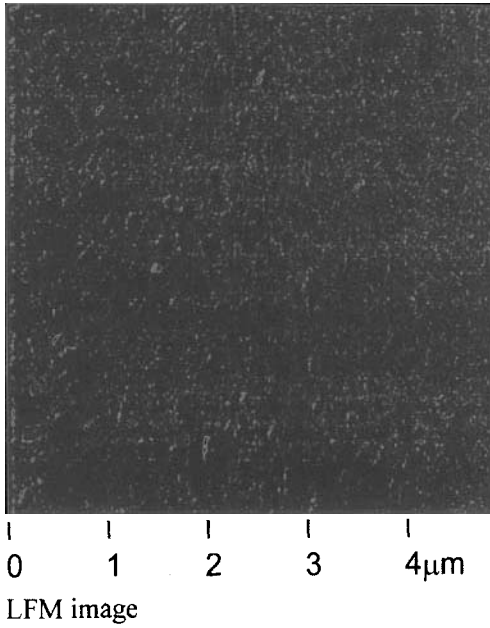
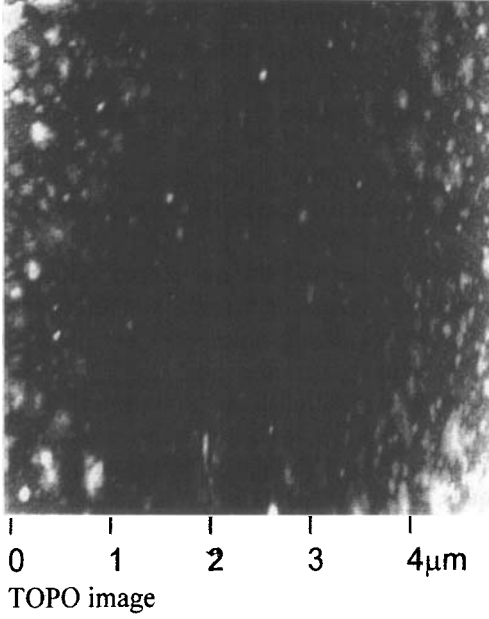


0 1 2 3 4 μm
LFM image

6b - Part 2

FIGURE 6 (Continued)

(b) 5 ML PI, APS, SiO_x



6b - Part 3

FIGURE 6 (Continued)

covered by PI. A closer inspection of Figure 6b also reveals that the protrusions do not serve as nucleation sites for the polymer islands. We suggest that the additional features on the APS-treated surface are polycondensates of aminosilane, which were formed during the imidization process in the presence of the PI precursor films. For bare APS MLs, dewetting and polycondensation during heat treatment in vacuum was not observed.

Before we conclude this report with a “post mortem” XPS analysis of delaminated PI films prepared by spin coating, we summarize the data obtained with the LB deposited films.

On both the native oxide and the APS surface, we find fragmentation and a deficit of oxydianiline, but a relatively higher concentration of pyromellitimide units on the aminosilane surface. We can not identify any specific chemical bonds between PI and aminosilane. These observations are consistent with chemical reactions between polyamic acid and aminosilane resulting in imide linkages as proposed by Greenblatt⁶ and Buchwalter⁴. Such imide linkage would not be discernible in the NEXAFS or XPS data because of the presence of PI. Although amide formation can be identified by our spectroscopic techniques, it was not detected.

The pyromellitimide units show a preferential orientation in the films, changing with film thickness. A similar angular behavior of the C 1s and N 1s absorption spectra in ML PI films on SiO_x was observed by Schedel-Niedrig¹³. Molecular order is not consistent with the notion of adhesion promotion by a higher degree of disorder and entanglement in the interphase in the presence of aminosilane. Rather, the molecular order observed in our data implies a higher density and cohesion within the PI interphase on SiO_x and aminosilane-treated surfaces, contrary to the observations on clean hydrophobic silicon³.

The polymer layers formed by imidization are not homogeneous. The morphology of PI islands is the same on both the SiO_x and APS surfaces. The aminosilane polycondensate protrusions on the APS-treated surface are coated with PI in the 5 ML films and might hence facilitate additional bonding by chemical bonds and mechanical interlocking between polymer and substrate on a mesoscopic scale. We also suggest that PI is present on the SiO_x and APS surface on the (flat) substrate areas in the AFM topographs because if PI is not present additional contrast in the lateral force images should have been observed. However, the protrusions on the APS surface do not act as nucleation sites for PI, and hence do not appear to have a high chemical reactivity towards the PI precursor. If the protrusions have a role in adhesion promotion, it appears to be by mechanical interlocking.

3.2 Delamination Experiments

It remains to be shown whether the AFM results on LB-deposited PI films have any significance for adhesion in spun-on films. However, if there is a component of mechanical interlocking between silane polycondensates and PI, some adhesion promotion effect should also be observed when methyl terminated alkylsilane MLs are applied instead of aminosilanes. We made some preliminary experiments with 2 μm spin-coated PI films on six different silane ML films: APS, AHTMS, n-Triacontyltrichlorosilane (TCTS), OTS, OTMS and PTS. Although our results on these ML films

are not necessarily directly comparable with work with multilayer silane deposits, we show here preliminary results for APS, OTS and PTS.

Attempts to delaminate these films with standard peel tests using Cr/Cu deposition onto the polymer surface for peeling failed on *all silane treated samples* due to the strong adhesion at the PI/silane/SiO_x interface; no, or only very weak, adhesion was observed between the bare SiO_x surface and the polymer. Therefore, the wafers were broken and partly peeled around the cleavage line. Small spot Si 2p, C 1s and N 1s XPS data were recorded on the SiO_x side of the laminates to determine the locus of rupture in the interphase. In Figure 7 we show representative data for APS, and the methyl-terminated silanes OTS and PTS.

The locus of failure in all cases was estimated from the intensity of the Si 2p XPS signal relative to the intensity of an untreated SiO_x surface to be 1.5–4 nm away from the silicon surface, *i.e.* somewhere in the vicinity of the silane/PI interface. In the XPS spectra, we detect some intensity characteristic for carbonyl carbons around $E_B = 289$ eV in the C 1s data and a small but significant N 1s intensity originating from PI fragments. The nitrogen signal could originate from the amino-terminated silane, but this is not possible in the case of OTS or PTS. Hence, we conclude that for *both* aminosilane and methyl-terminated silane fracture occurs to some extent within the PI film.

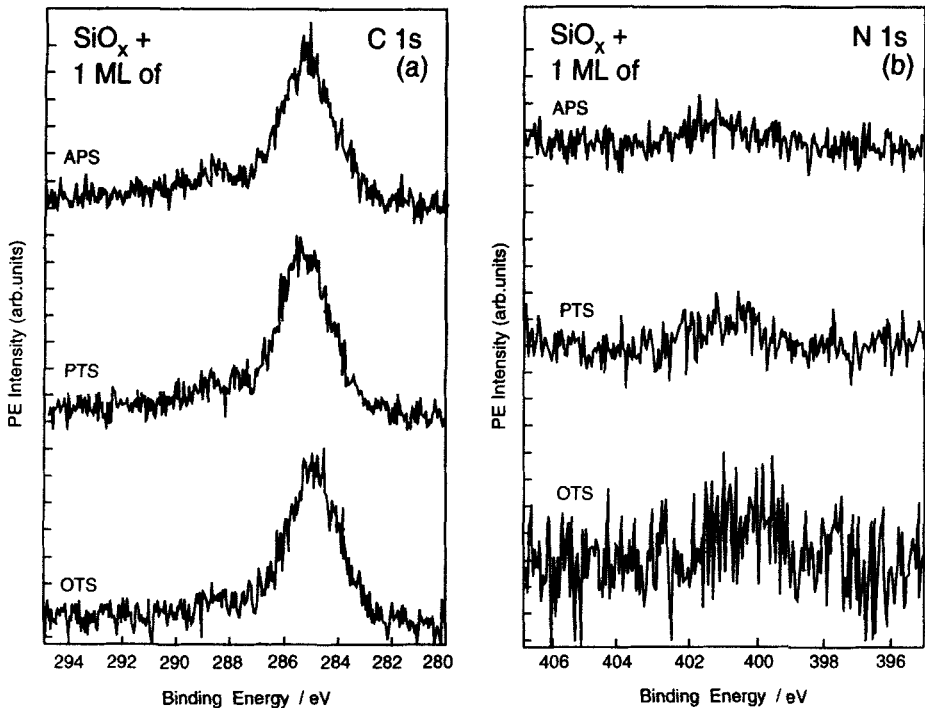


FIGURE 7 (a) C 1s and (b) N 1s data taken on the silicon side of delaminated, spun-on, PI films on SiO_x surfaces covered with a ML film of 3-aminopropyltriethoxysilane (APS), octadecyltrichlorosilane (OTS) and n-propyltrichlorosilane (PTS). See text for discussion.

We offer a possible explanation for the presence of PI residues on the SiO_x side of the laminate. If the methyl-terminated silane films dewet the surface, as seen in the AFM data for LB-deposited PI on the APS-treated surface, a direct contact is permitted between PI and the SiO_x substrate, which provides no or little adhesion. In view of the AFM data on the APS-treated surface, and the similar XPS data on the fracture surfaces, formation of OTS and PTS coagulates in the presence of polyamic acid and mechanical interlocking is a possible interpretation for the delamination results. However, no AFM data for LB-deposited polyamic acid films on OTS or PTS have been recorded so far. Further studies have to be done to verify our observation of good adhesion between PI and methyl-terminated alkylsilane films on silicon.

SUMMARY

Since, under the conditions of our study, we can not identify any specific chemical bonds between PI and the aminosilane ML, we conclude that, if they exist, only imide linkages are formed between the pyromellitimide unit of the polymer and the aminosilane coupling layer. Our data are consistent with the model proposed originally by Greenblatt for the APS surface⁶, *i.e.* polyamic acid reacts with the silane amine groups first to form amide linkages, which are thermally unstable and decompose under desorption of oxydianiline to form stable imide bonds between the pyromellitimide unit and the silane. Surprisingly, the same interpretation of the NEXAFS data with imide formation and desorption of oxydianiline fragments is applicable for the untreated SiO_x surface. Since macroscopic adhesion as measured in other work is weak between the untreated SiO_x surface and PI, but much stronger between the aminosilane treated SiO_x surface and PI, we conclude from our AFM data that mechanical interlocking between silane polycondensates and polymer on a mesoscopic scale contributes to macroscopic adhesion. Support for such a model is found in our delamination experiments of spun-on PI films on SiO_x surfaces treated with a variety of methyl-terminated silane films showing evidence for strong adhesion.

Acknowledgements

We thank M. Kinzler, W. Schrepp and J. Rogers for their help with some of the experiments. This work was supported by the Office of Naval Research and the BMFT (FKZ 055 VHFX 19).

References

1. F. Brochard-Wyart, P. G. de Gennes, L. Leger, Y. Marciano and E. Raphael, *J. Phys. Chem.*, **98**, 9405 (1994).
2. T. S. Oh, L. P. Buchwalter and J. Kim, *J. Adhesion Sci. Technol.*, **4**, 303 (1990).
3. M. Grunze, G. Hähner, Ch. Wöll and W. Schrepp, *Surf. Interface Anal.*, **20**, 393 (1993).
4. L. P. Buchwalter, *J. Adhesion Sci. Technol.*, **4**, 694 (1990).
5. T. S. Oh, L. P. Buchwalter and J. Kim Raphael, in *Acid-Base Interaction*, K. L. Mittal and H. R. Anderson, Eds. (VSP, Utrecht, 1991).
6. J. Greenblatt, C. J. Araps and H. R. Anderson, in *Polyimides: Synthesis, Characterization and Applications*, Vol. 1, K. Mittal, Ed. (Plenum Press, New York, 1984), p. 573.
7. A. Killinger, C. Thummler and W. Schrepp, *J. Adhesion*, **36**, 229 (1992).

8. M. Grunze, W. Meyer, R. Lamb, A. Ortega-Vilamil and W. Schrepp, *Surf. Sci.*, **273**, 205 (1992).
9. M. Grunze, M. Buck, Ch. Dressler, and M. Langpape, *J. Adhesion*, **45**, 227 (1994).
10. K. Bierbaum, G. Hähner, S. Heid, M. Kinzler, Ch. Wöll, F. Effenberger and M. Grunze, *Langmuir*, **11**, 512-518 (1995).
11. K. Bierbaum and M. Grunze, Proc., The Adhesion Soc., 17th Ann. Meeting, p. 213 (1994).
12. K. Bierbaum, M. Grunze, A. A. Baski, L. F. Chi, W. Schrepp and H. Fuchs, *Langmuir*, **11**, 2143 (1995).
13. Schedel-Niedrig, Dissertation, T. U. Berlin (1994).
14. J. Stöhr, *NEXAFS Spectroscopy*, Springer Ser. Surf. Sci., Vol. 25 (Springer, Berlin, Heidelberg, etc. (1992).